Supplementary of

Chemical evolution of secondary organic aerosol tracers during high $PM_{2.5}$ episodes at a suburban site in Hong Kong over 4 months of continuous measurement

Q. Wang et al.

Correspondence to: Jian Zhen Yu (jian.yu@ust.hk)

Text S1. General characteristic and $PM_{2.5}$ level at the 15 HKEPD air quality monitoring stations

1.1 Site characteristic

The air quality monitoring network in Hong Kong was operated by Hong Kong Environment Protection Department (HKEPD), which provides public information on current and forecasts air quality, containing 15 general stations and 3 roadside stations. Table S1 shows the site characteristics of the 15 HKEPD general air quality monitoring stations and the HKUST supersite, and Figure S1 shows the geographical locations. Among the 15 HKEPD stations, 10 are in New Territories (i.e., NH, ST, TP, YL, TM, TC, TW, KC, TK, MB), 2 in Kowloon (i.e., SP and KT), and 3 in Hong Kong Island (i.e., CW, EN and SN). One station, MB, is a rural site located on the isolated grass island in the northeastern HK and can be regarded as a background site. Others are general urban sites with different microenvironments and among them 6 are located in the new town area in the northern/northwestern area of HK (i.e., NH, ST, TP, YL, TM, and TC).

Table S1. Site characteristics of the 15 HKEPD general air quality monitoring stations and the HKUST supersite.

Station	Abbreviation	Latitude (°)	Longitude (°)	District	Type
North	NH	22.50	114.13	New Territories	New Town
Sha Tin	ST	22.38	114.18	New Territories	New Town
Tai Po	TP	22.45	114.16	New Territories	New Town
Yuen Long	YL	22.45	114.02	New Territories	New Town
Tuen Mun	TM	22.39	113.98	New Territories	New Town
Tung Chung	TC	22.29	113.94	New Territories	New Town
Tsuen Wan	TW	22.37	114.11	New Territories	Urban
Kwai Chung	KC	22.36	114.13	New Territories	Urban
Sham Shui Po	SP	22.33	114.16	Kowloon	Urban
Kwun Tong	KT	22.31	114.22	Kowloon	Urban
Central/Western	CW	22.29	114.14	Hong Kong Island	Urban
Eastern	EN	22.28	114.22	Hong Kong Island	Urban
Southern	SN	22.25	114.16	Hong Kong Island	Urban
Tseung Kwan O	TK	22.32	114.26	New Territories	Urban
Tap Mun	MB	22.47	114.36	New Territories	Rural
HKUST supersite	HKUST	22.33	114.27	New Territories	Rural

Figure S1. Geographical location of the 15 HKEPD general air quality monitoring stations and the HKUST supersite, with new town stations shown in grey icons, urban stations in blue icons and rural stations in red icons (map data: © Google Earth, TerraMetrics Maxar Technologies Data SIO, NOAA, U.S. Navy, NGA, GEBCO, Image Landsat/Copernicus CNES/Airbus).

1.2 PM pollution feature

Figure S2 shows the statistics of the $PM_{2.5}$ level among the 15 HKEPD stations and the HKUST site in different seasons (The separation of different seasons are discussed in Text S3). Generally, PM levels were low and comparable among all sites in summer, while the PM levels in fall and winter elevated with larger spatial variability. Among the new town stations, TM always showed the highest PM level, while among the stations in urban residential areas, TW, KT, and CW were the three leading stations. It can be seen that in winter, the PM levels at two rural sites MB and HKUST were comparable to or even higher than those at some urban stations (e.g., KC, SP, SN and TK), suggesting the importance of regional transport influence in winter.

Figure S3 shows the site-by-site correlation of the $PM_{2.5}$ level among the 15 HKEPD stations during the study period (10 Jul.-31 Dec. 2020), separated by the episodic and non-episodic periods. Generally, $PM_{2.5}$ concentrations varied synchronously among different sites, regardless of urban or background sites (i.e., MB), with correlation coefficient (R_p) ranging 0.71-0.92 during the non-episodic period, suggesting the regional characteristics of PM pollution in HK (Figure S3a). While under the episodic period, poorer correlations were observed, signifying the spatial heterogeneity of the PM episode formation at the city scale (Figure S3b).

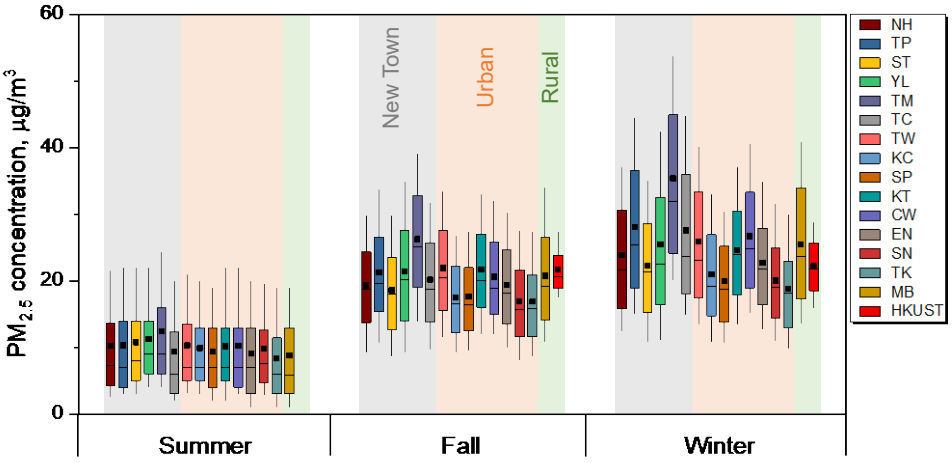

Figure S2: Box plot of the $PM_{2.5}$ concentration among the 15 HKEPD general air quality monitoring stations and the HKUST supersite during 10 Jul.-31 Dec. 2020 (squares and solid lines correspond to mean and median values, respectively; boxes indicate the 25th and 75th percentile, and whiskers are the 10th and 90th percentile).

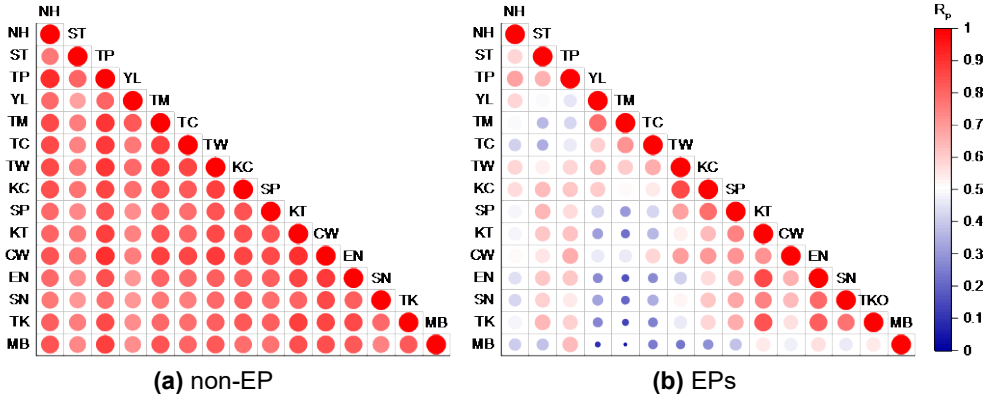

Figure S3: Site-by-site correlation (R_p) of $PM_{2.5}$ among the 15 HKEPD air quality monitoring stations for (a) non-episodic period and (b) episodic period during 10 Jul.-31 Dec. 2020.

Text S2. Correction of $PM_{2.5}$ at HKUST and treatment of missing data

2.1 RH and $PM_{2.5}$ correction

During the sampling period, negative bias was observed for the RH measurement with the old sensor, evidenced by the measured RH value lower than 90% during the precipitation events (Figure S4 upper right panel). To correct the RH data, we compared the measured RH with the parallel RH&T measurement by a new sensor adopted from Mar. to Apr. 2021 to obtain

the correction parameters. Temperature showed no bias with R^2 of 0.999 and slope of close to 1. While power relationship was observed between the RH values from two sensors (Figure S4 upper left panel). The power function in Eq. 1 was used to correct the measured RH during this campaign period:

$$RH_{corrected} = \left(RH_{old\ sensor} \times \frac{1}{0.004}\right)^{\frac{1}{2.1702}} \quad (1)$$

During the sampling period, the Sharp Monitor measured $PM_{2.5}$ data were biased, with the $PM_{2.5}$ concentrations lower than the summed speciation data. 24-h offline filter measurement was conducted once-every-six-day during the campaign period. The Sharp measured $PM_{2.5}$ showed good linear correlation with the offline filter measurement (Figure S4 lower left panel), making it feasible to use the offline filter data to correct the Sharp measured $PM_{2.5}$ (Eq. 2). The corrected $PM_{2.5}$ are closer to offline filter-based $PM_{2.5}$ data and showed better mass closure with the speciation measurement (Figure S4 lower right panel).

$$PM_{2.5,corrected} = (PM_{2.5} + 0.3558) \times \frac{1}{0.5283} \quad (2)$$

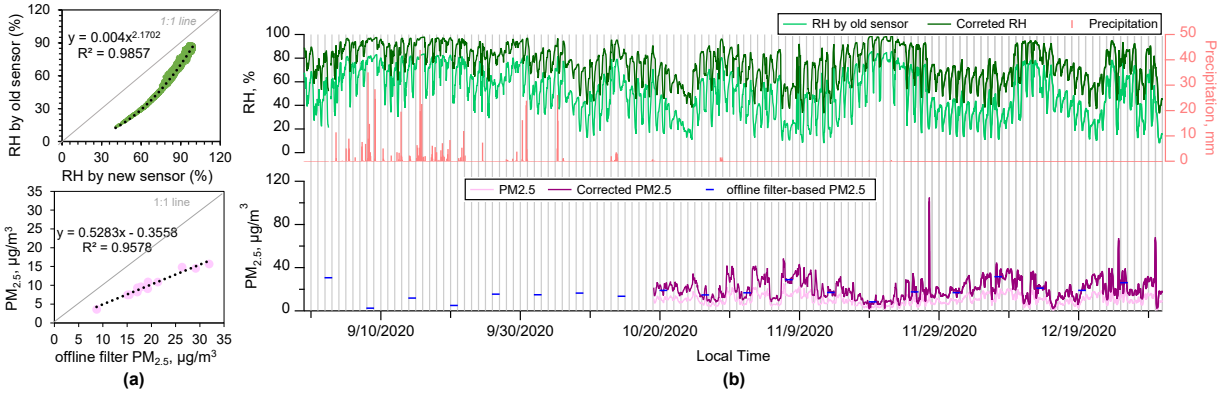

Figure S4: (a) Power relationship was observed between the RH measured by the old sensor and the RH by the new sensor during Mar. to Apr. 2021 at HKUST supersite (upper left panel) and linear relationship between online and offline filter-based $PM_{2.5}$ data during 8/30/2020-12/31/2020 (lower left panel). (b) Time series of RH by the old sensor and the corrected RH (upper right panel), and measured hourly $PM_{2.5}$ by Sharp Monitor, the corrected $PM_{2.5}$ and the offline filter-based $PM_{2.5}$ during 8/30/2020-12/31/2020 at HKUST supersite (lower right panel).

2.2 Treatment of missing data for O_3 and $PM_{2.5}$

The gas pollutants (i.e., O_3, SO_2 and NO_x) and $PM_{2.5}$ measurement at HKUST supersite were not available during 8/30-9/21 and 8/30-10/18, respectively (Figure S5). Among the 15 HKEPD air monitoring stations, TK station is a general urban station which is closest to HKUST supersite, with the distance of ~1.8 km. On the other hand, MB station is a rural station, with less local emission sources and the surroundings are more similar to that of HKUST. The distance between MB and HKUST site is 10 km. We compared the ozone and $PM_{2.5}$ concentrations among the three stations (Figure S5). High correlations were observed among the three stations for both $PM_{2.5}$ and O_3 for the remaining time period (R_p of 0.78-0.88), and the concentrarions

at MB station were closer to that at HKUST (slope of 0.94 for O_3 and 0.88 for $PM_{2.5}$). Thus, for the missing periods, $PM_{2.5}$ and O_3 concentration at MB station were used as reference in the analysis.

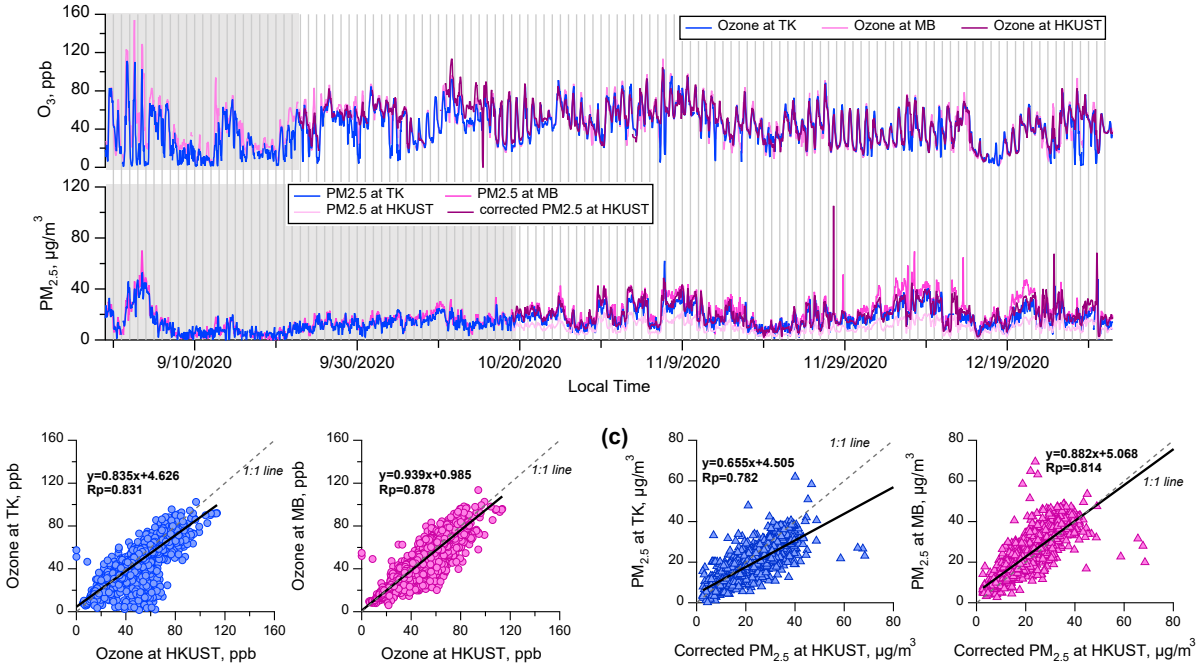

Figure S5: (a) Time series of ozone and $PM_{2.5}$ at HKUST, TK, and MB stations during 8/30-12/31, 2020, with grey area showing the time period when the measurement data at HKUST is not available. (b) Scatter plot of avaible ozone at TK and MB vs. HKUST during the remaining time period. (c) Scatter plot of avaible $PM_{2.5}$ at TK and MB vs. HKUST during the remaining time period.

Text S3. Seasonal division

HK and the rest of PRD region are situated in the sub-tropics. The seasonal evolution of weather in HK is closely related to and controlled by seasonal evolution of the East Asian Monsoon system. In this study, the upper-level wind direction, one of the best indicators for seasonal change around HK, is used to reflect the seasonal variation in HK (Yu, 2002). The sea-level pressure and the dew point are used to pinpoint the exact dates of the seasonal divisions, i.e., the arrival date of the first synoptic event that is typical in the respective seasons. Figure S6 shows the time series of the upper wind direction, sea-level pressure and dew point during the study period (7/10-12/31, 2020). The study period was divided into three seasons, i.e., summer (Jul. 10-Oct. 7), fall (Oct. 8-Nov. 28) and winter (Nov. 29-Dec. 31). In summer, HK was mainly influenced by the southern oceanic air mass, while in fall and winter northern continental air mass dominated (Figure S7).

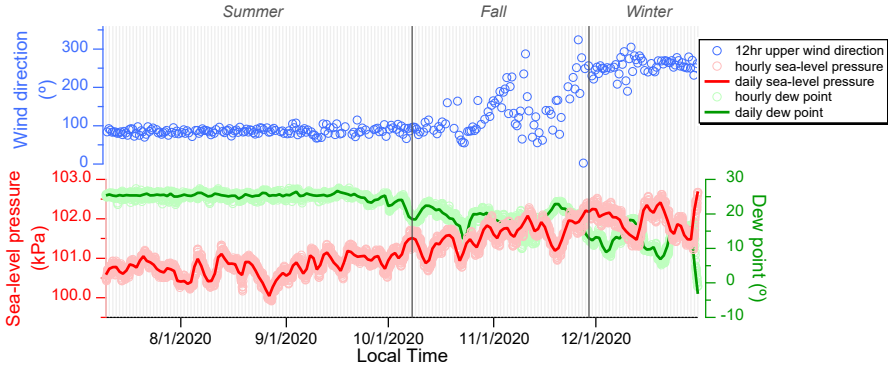

Figure S6: Criteria for season division in this study. Upper panel: time series of wind direction at 20000±1000 m height. Lower panel: time series of the sea-level pressure and dew point at Hong Kong Observatory station over the course of the study period (Jul. 10 – Dec. 31, 2020).

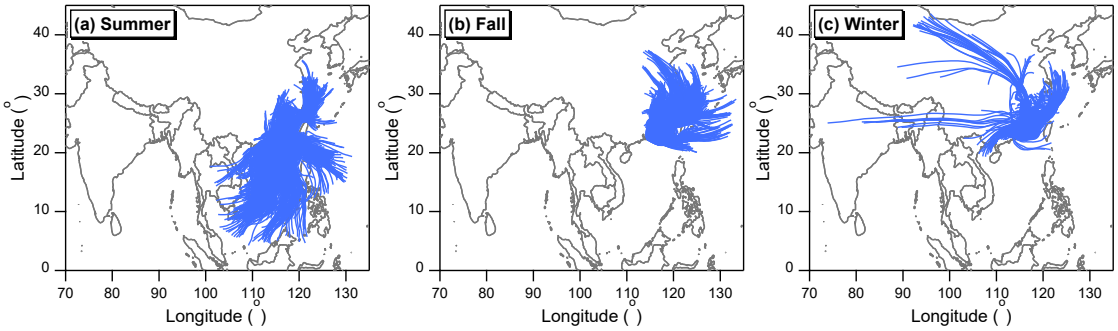

Figure S7: The 72-h backward trajectories arriving at HKUST supersite (22°20'N, 114°16'E) at an elevation of 500 m for (a) summer, (b) fall, and (c) winter.

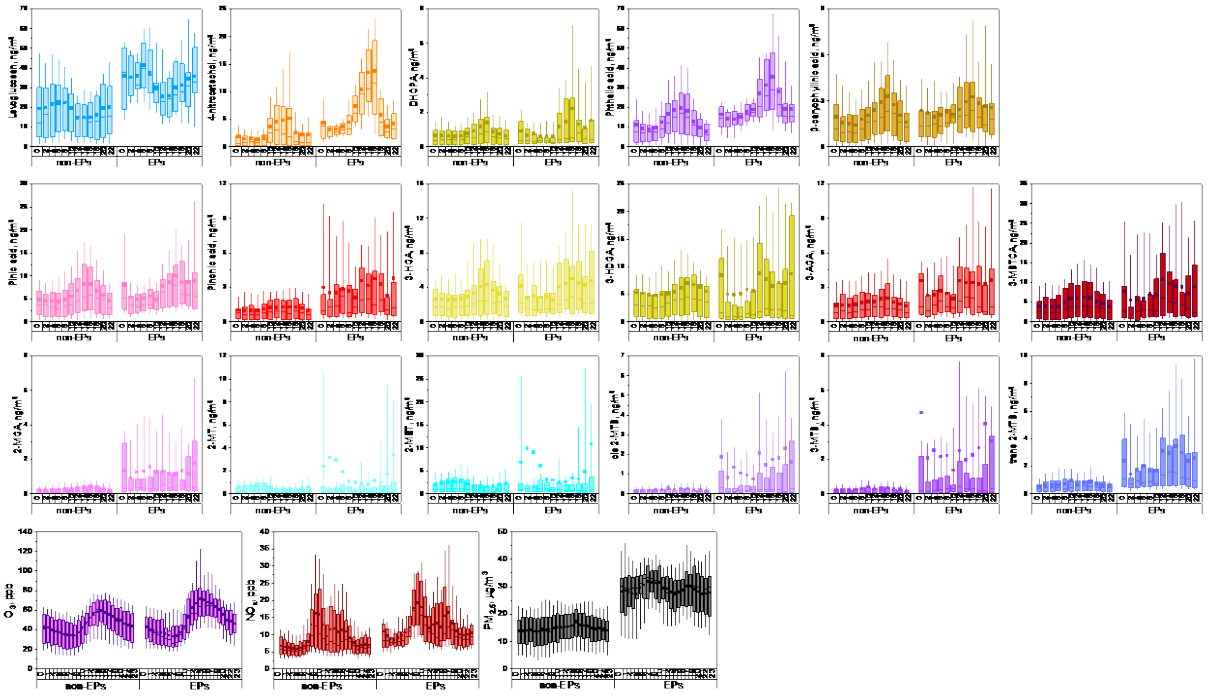

Figure S8: Diurnal variations of (a) levoglucosan, 4-nitrocatechol, DHOPA, phthalic acid, and β-caryophyllinic acid; (b) individual α-pinene SOA tracers; (c) individual isoprene SOA tracers, and (d) O_3 , NO_x and $PM_{2.5}$ under the non-episodic and episodic period from 8/30-12/31, 2020 at HKUST supersite.

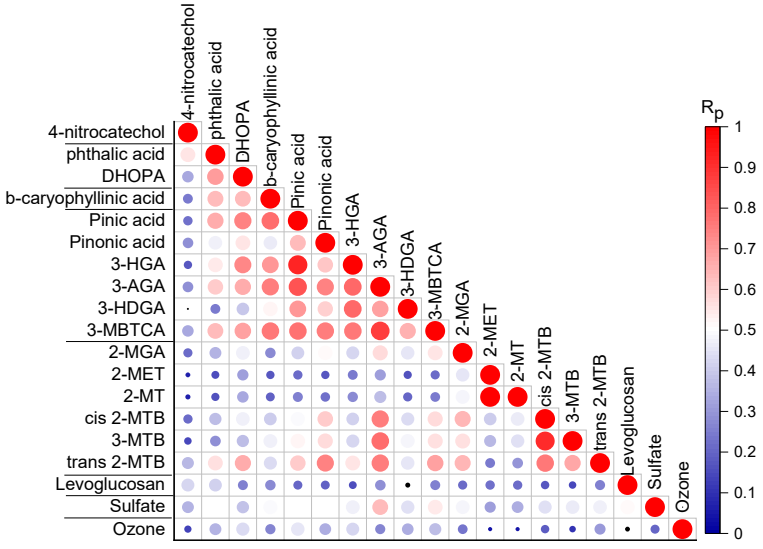

Figure S9: Inter-species correlation (R_p) among individual SOA tracers and sulfate and ozone measured at HKUST supersite during 8/30-12/31, 2020.

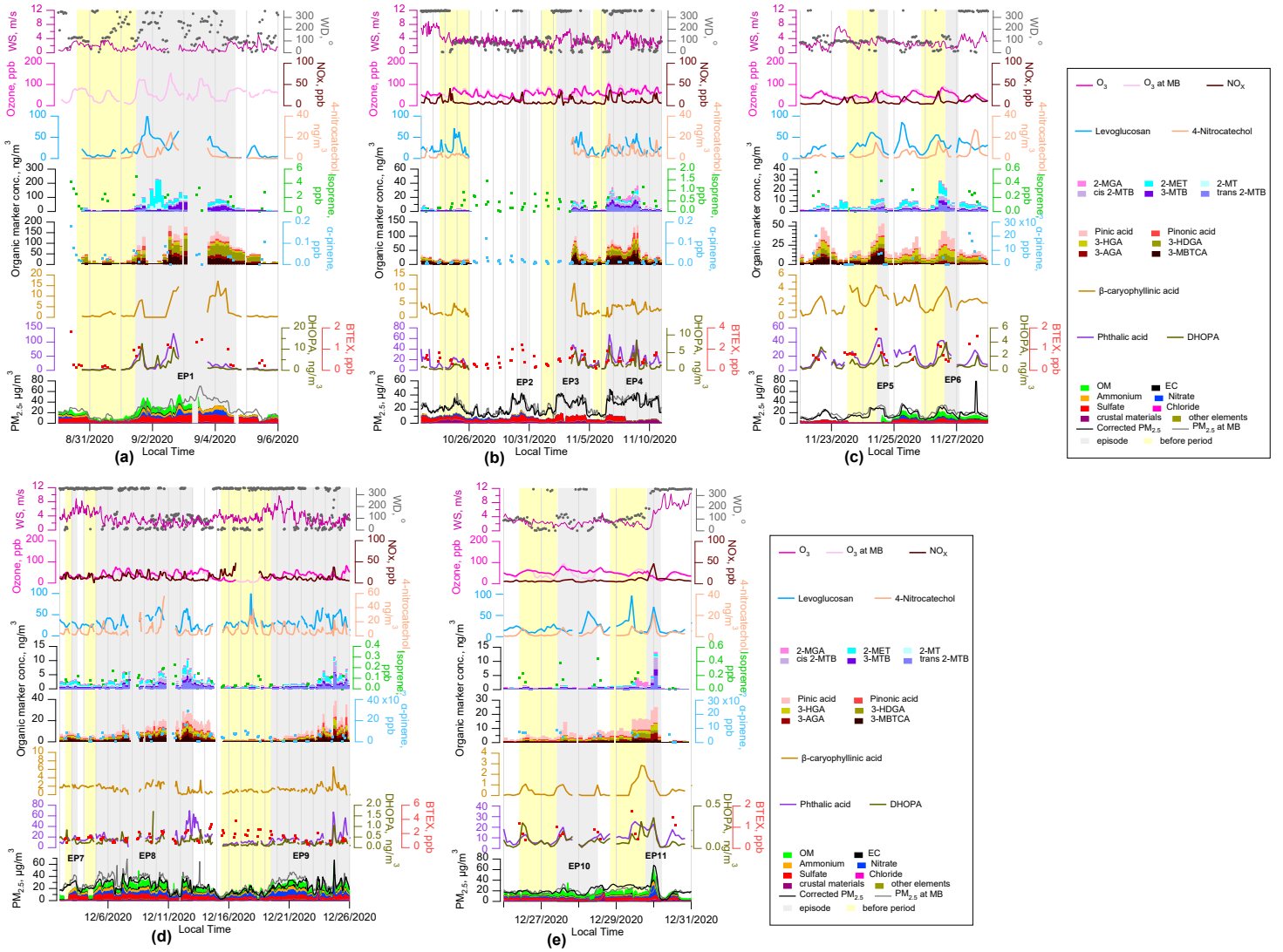

Figure S10: Time series of $PM_{2.5}$ and its major components and select SOA tracers for individual episodes (gray shaded) and its before period (yellow shaded): (a) EP1, (b) EP2, 3 and 4, (c) EP5, and 6, (d) EP7, 8 and 9, and (e) EP10 and 11 during 8/30-12/31,2020 at HKUST supersite.

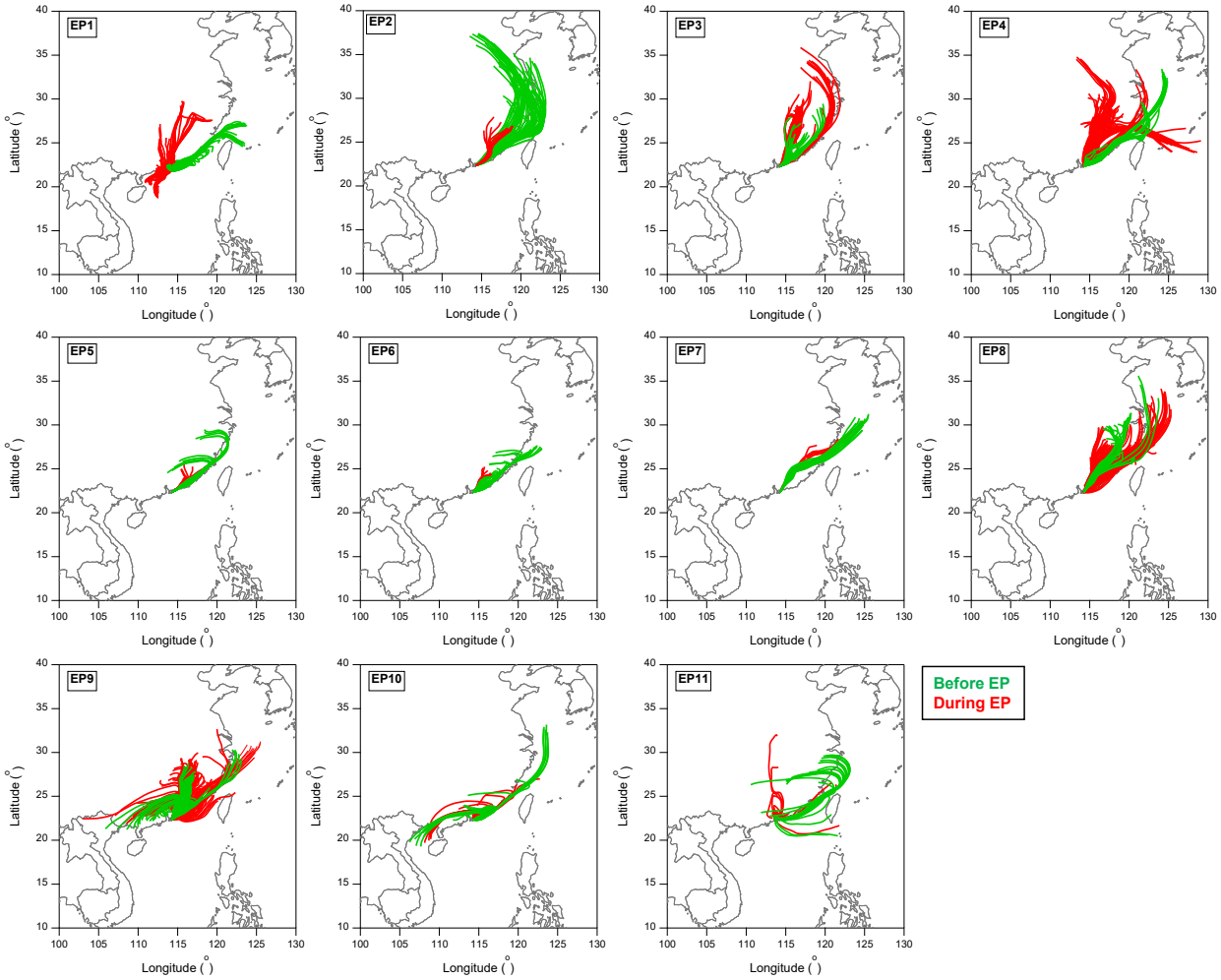

Figure S11: The 72-h backward trajectories arriving at HKUST supersite (22°20'N, 114°16'E) at an elevation of 500 m for each episode and its before period.

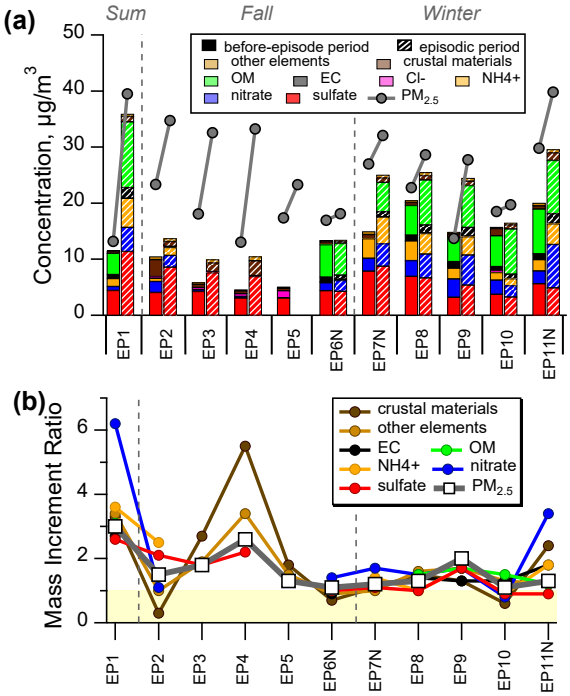

Figure S12: (a) Average concentrations of $PM_{2.5}$ and its major components during the before (solid filling) and episodic period (pattern filling), and (b) the mass increment ratio of individual component for each episodes, with the light-yellow area marking the ratio values less than 1.

Table S2: Summary of meteorological conditions and gas pollutants before and during each episode measured at HKUST site during 8/30-12/31, 2020.

Episode		Time period	Duration (h)	$PM_{2.5}$ ($\mu g/m^3$)	Mixing Height (m)	RH (%)	Temp (^oC)	Wind speed (m/s)	Air mass origins$^{\perp}$	O_3 (ppb)	SO_2 (ppb)	NO (ppb)	NO_x (ppb)
EP1	Before	8/30 2:00 PM-9/1 11:00 AM	46	12.5	289.6	73.8	29.2	1.78	Coastal	39.0	/	/	/
	During	9/1 12:00 PM - 9/4 3:00 PM	76	37.5	239.0	78.0	29.7	1.33	Mixed	63.4	/	/	/
EP2	Before*	10/23 1:00 PM-10/26 0:00 AM	60	22.2	282.4	59.3	22.8	3.71	MR-NE	64.3	1.09	5.42	10.2
	During	10/30 7:00 AM - 10/30 7:00 PM	13	33.0	765.0	79.0	23.2	2.72	SR-NE	48.5	0.28	13.1	12.6
EP3	Before	11/1 12:00 AM-11/2/ 6:00 AM	31	17.2	282.4	73.9	22.3	2.38	MR-NE	60.6	0.61	0.44	5.66
	During	11/2 7:00 AM - 11/4 9:00 PM	63	31.0	357.6	65.5	23.2	3.93	MR-NE	57.6	1.12	8.43	12.0
EP4	Before	11/5 8:00 AM-11/6 10:00 AM	27	12.4	358.4	73.0	22.0	2.47	MR-NE	55.7	0.45	4.19	7.03
	During	11/6 11:00 AM -11/10 10:00 PM	108	31.6	367.4	56.9	24.2	3.36	MR-NE	69.0	2.16	5.44	13.1
EP5	Before#	11/23 12:00 PM-11/24 11:00 AM	24	16.5	194.7	86.9	21.3	2.84	MR-NE	35.8	0.12	8.59	10.8
	During	11/24 12:00 PM -12/24 7:00 PM	8	22.1	893.4	79.1	22.4	3.44	SR-NE	58.4	0.30	3.77	8.22
EP6N	Before	11/25 9:00 PM-11/26 3:00 PM	19	16.1	350.4	77.4	23.4	2.41	MR-NE	51.7	0.34	8.50	10.2
	During	11/26 4:00 PM -12/27 1:00 AM	10	17.2	278.9	89.6	20.8	1.36	SR-NE	58.5	0.20	0.50	7.20
EP7N	Before	12/2 11:00 AM-12/3 0:00 AM	14	25.6	508.7	57.0	20.9	3.78	MR-NE	40.2	1.08	16.0	17.3
	During	12/3 1:00 AM -12/3 10:00 AM	10	30.5	19.2	67.7	15.6	6.13	MR-NE	26.2	1.06	6.63	11.2
EP8	Before	12/4 2:00: AM-12/5 1:00 AM	24	21.6	141.9	61.3	15.0	5.32	MR-NE	29.9	0.77	11.2	14.2
	During	12/5 2:00 AM -12/12 11:00 PM	191	27.2	284.8	71.5	18.7	2.59	MR-NE	41.8	1.08	5.45	13.9
EP9	Before	12/15 8:00 AM-12/19 12:00 PM	101	13.0	149.3	69.5	13.7	3.70	Mixed	15.2	0.23	19.43	22.1
	During	12/19 1:00 PM -12/25 10:00 PM	154	26.3	295.2	68.0	16.3	3.62	Mixed	38.1	1.32	2.54	11.3
EP10	Before	12/26 10:00 AM-12/27 10:00 AM	25	17.6	310.5	76.7	18.5	2.27	MR-NW	53.8	0.81	0.77	5.58
	During	12/27 11:00 AM -12/28 11:00 AM	25	18.7	353.0	58.0	20.5	1.89	MR-NW	61.7	1.42	0.88	6.69
EP11N	Before#	12/28 8:00 PM-12/29 7:00 PM	24	28.3	344.8	76.8	19.4	2.06	MR-NE	48.3	0.59	3.94	9.04
	During	12/29 8:00 PM -12/30 4:00 AM	9	37.8	75.4	72.1	18.5	3.70	Mixed	32.2	1.61	0.57	21.3

* the selected time window to be comparable with that of the EP3, as no organic data for its before period.

the selected 1d time window to cover the corresponding daytime/nighttime hours for the episode.

$^{\perp}$ MR-middle range; SR-short range; NE-northeastern; NW-northwestern.

Reference

Yu, J. Z.: Chemical Characterization of Water Soluble Organic Compounds in Particulate Matters in Hong Kong. Environmental Protection Department, 2002. Retrieved from https://citeseerx.ist.psu.edu/viewdoc/download?doi=10.1.1.562.1645&rep=rep1&type=pdf